Available online at www.sciencedirect.com
SCIENCE DIRECT®
ELSEVIER
C. R. Physique 6 (2005) 1110–1117
COMPTES RENDUS
PHYSIQUE
http://france.elsevier.com/direct/COMREN/

MCAO for very large telescopes/OAMC pour les très grands télescopes

FALCON: multi-object AO

Eric Gendron [a,*], François Assémat [a], François Hammer [a], Pascal Jagourel [a], Fanny Chemla [a], Philippe Laporte [a], Mathieu Puech [a], Michel Marteaud [a], Frédéric Zamkotsian [b], Arnaud Liotard [b], Jean-Marc Conan [c], Thierry Fusco [c], Norbert Hubin [d]

[a] *Observatoire de Paris, 5, place Jules Janssen, 92195 Meudon cedex, France*
[b] *Laboratoire d'astrophysique de Marseille, UMR 6110, 2, place le Verrier, 13248 Marseille cedex 4, France*
[c] *Onera, BP72, 29, avenue de la division Leclerc, 92322 Châtillon cedex, France*
[d] *European Southern Observatory, Karl-Schwarzschild-Strasse 2, 85748 Garching bei München, Germany*

Abstract

FALCON is a wide-field, multi-object integral field spectrograph equipped with adaptive optics. It is dedicated to the study of the formation process of primordial galaxies. The AO system uses natural guide stars, and the high sky coverage required for these studies is obtained using tomographic techniques for the wavefront analysis. The structure of the OA system is very new, and particularly suited for a future implementation on extremely large telescopes. ***To cite this article: E. Gendron et al., C. R. Physique 6 (2005).***

Résumé

FALCON : optique adaptative multi-objet. FALCON est un spectrographe intégral de champ multi-objet grand champ équipé d'une Optique Adaptative (OA). Ce système est dédié à l'étude de la physique de la formation des galaxies primordiales. Le système d'OA utilise des étoiles naturelles, et la grande couverture de ciel requise pour ce type d'étude est obtenue en utilisant une approche tomographique pour l'analyse de front d'onde. La structure très novatrice de ce système d'OA est particulièrement attractive pour équiper les futurs télescopes extrêmement grands. ***Pour citer cet article : E. Gendron et al., C. R. Physique 6 (2005).***

Keywords: Adaptive optics; Spectroscopy

Mots-clés : Optique adaptative ; Spectroscopie

1. Introduction

Progress in the field of galaxy formation and cosmology has accelerated in the past 10 years. It is now widely believed that galaxies are formed by the cumulative accretion of smaller units during the whole Universe age, in the frame of the 'hierarchical

* Corresponding author.
E-mail address: eric.gendron@obspm.fr (E. Gendron).

1631-0705/$ – see front matter © 2005 Académie des sciences. Published by Elsevier SAS. All rights reserved.
doi:10.1016/j.crhy.2005.10.012

galaxy formation' scenario. A major goal of modern astrophysics is now to understand our origin, i.e. the physical processes of the formation of stars and metal in galaxies, which ultimately lead to the formation of telluric planets and life. The main steps required to answer this fundamental question can be described as it follows:

– identify the first seeds formed in the Universe before re-ionization, at a stage when the Universe was mainly under the form of an almost homogeneous gas phase;
– describe which objects (galaxies, QSOs, ultra-massive stars) are the main responsible for the re-ionization of the Universe at an age of less than 1 Gyr ($z = 8$–15), i.e. of the change from a mainly neutral and opaque Universe, to the Universe at $z = 2$–5 which was mostly dominated by ionized gas species;
– understand the complex physics which governs the galaxy assembly from the first seeds, involving the relationship between the assemblies of baryonic matter – gas transformed into stars – and dark matter, respectively.

These investigations are facing several challenges, which are related to the nature of distant objects and galaxies:

– galaxies in the past appear to be extremely faint sources which results from the combination of their very large distances ($> 10^{10}$ light years) and their intrinsic faintness; besides this, most of their emission is redshifted to the near and mid-infrared;
– galaxies in the past were much smaller than those at present-day, with typical angular size of 0.25 arcsecond at $z = 3$ to 0.15 arcsecond at $z = 7$–8;
– the investigation of galaxy kinematics, gas chemistry and stellar populations should be done at relatively high spectral resolution, because distant galaxies are kinematically small (few tens of km/s) and that gas chemistry and star formation process require a resolution down to the scale of giant HII regions or molecular clouds (few km/s);
– the complexity of galaxy assembling requires a full diagnostic of all the process from the center to the outskirt gas in the halo, i.e. its study requires a well spatially and spectrally resolved 3D spectroscopy [1];
– galaxies and massive objects in the Universe belong to large structures and are correlated over typical scales of 4 to 9 Mpc [2,3], which correspond to angular sizes over 10 arcminutes on the sky at $z \gg 1$.

These typical requirements are far beyond the present generation of telescopes [4]. Space experiments such as the James Webb Space telescope (JWST) would be exquisite in detecting very faint and distant sources, although it cannot accommodate for high resolution spectroscopy with 3D devices and would operate only with modest fields of view (few arcminutes). Without spectroscopic information, one can only learn a limited amount about the basic properties of the distant objects.

However, the major challenge for the ground based telescopes is to overcome atmospheric turbulence, which leaves us with image qualities of 1.0 to 0.5 second of arc, at very best, for long exposures. It can be corrected by the mean of adaptive optics, which is currently able to resolve sizes well below 0.1 arcsecond at an 8 meter telescope (e.g. NACO on VLT) if there is a bright star near the object (at less than 20 arcseconds, e.g. the isoplanetism diameter [5]) which is used at a reference for correcting the turbulence. However, such systems can only correct a very limited fraction of the sky (far less than 1%) because of the scarcity of bright stars, especially for cosmological fields which lie far away from the plane of our Galaxy.

We are investigating an original concept, that we called FALCON, which aims at extending adaptive optics corrections over very large fields with a high sky coverage, in order to simultaneously observe 15 to 20 objects, and benefit from the multiplex gain. The observation of a very large number of objects is mandatory in our studies, that rely on a statistical approach. The principle of FALCON is to optimize the correction at the specific tiny areas of the sky where the distant science objects are laying, within the huge field of view of 25 arcminutes of the VLT.

In the following section we describe the FALCON concept, and focus on particular technical challenges. Section 3 details the simulations we performed in order to derive the performance of such an instrument. We show how we took into account the tomographic aspects, whose performance is closely related to the guide star density. We also discuss the parameters of the AO-corrected image, that are most relevant for 3D-spectroscopy.

2. FALCON adaptive optics system

2.1. Why MCAO is not suitable

An overall look at the current state-of-the-art of adaptive optics shows a class of instruments, that aim at correcting wide fields of view, while increasing the sky coverage: they are Multi-Conjugate Adaptive Optics systems (MCAO systems) [6–9]. This technique consists in:

– sensing the wavefront disturbances across the field of view, in order to reconstruct the phase disturbance in the full volume above the pupil; this is called 'tomography' [10–12];
– compensating the phase in a 3D fashion, using several deformable mirrors along the light path and conjugated with the turbulent layers.

This technique is very effective at increasing the size of the compensated field of view. However, all the instruments of this type, and those currently in development, foresee compensated fields of, at best, only 2 arcminutes in diameter (see instruments called MAD at ESO [13], or GEMINI MCAO system [14]). This field of view is still an order of magnitude below what we need. Of course, those systems aim to approach a diffraction-limited correction, and this is partly because of technical challenges that they have to limit the field to such a value. Considering that we only need a moderate compensation, we could expect to extend it a bit further – 4 to 5 arcmin. In any case, such a wide field of 25 arcmin would increase the size of the MCAO instrument and the size of its optical components to a totally unreasonable amount. Let us have a rough estimate of the dimensions of such a system: as we will see in the last sections of this article, we need deformable mirrors with approximately 70 degrees of freedom in the pupil; assuming the use of 4 piezostack or bimorph mirrors, this implies pupil sizes of about 80 mm. A distance of 1 km between conjugated layers then translates into 0.1 m on the bench, while the 25 arcminutes translate into a beam angle of 42 degrees. The size of the 10 km-conjugated mirror should be approximately 80 cm in diameter. The optics of such a system is just inconceivable.

2.2. FALCON concept versus GLAO

GLAO stands for ground-layer adaptive optics. A GLAO system [18] compensates for the turbulence located between the ground and a maximum altitude of – typically – a few tens of meters. This altitude depends on the width of the field to be compensated. The larger the field of view, the smaller will be the thickness of the compensated layer. Assuming that an actuator spacing of 80 cm is required for a proper phase compensation, the highest layer that can efficiently be compensated with a 25 arcmin fov is such that the projections of the pupil on this layer for 2 opposite edges of the field will differ from, let us say, half the actuator spacing. In our case, the result is an altitude of 50 meters (let us notice this number is independent of the telescope diameter).

The integrated $C_n^2(h)$ on the first 50 meters is negligible (at least, in Paranal) compared to the whole phase variance. This means that the GLAO efficiency is marginal for a 25 arcmin field. This would be wrong for smaller field, i.e. 2 arcminutes, and shows that a concept like FALCON is reserved for very wide fields.

Moreover, the pupil in the VLT is formed by the secondary mirror. The entrance pupil of the telescope is the image of the secondary mirror through the primary one. This entrance pupil is a virtual one, located 90 meters below the ground. In other words, as layer heights are to be counted from the pupil, the turbulence located at the very ground level must be considered at an altitude of 90 m. This definitely excludes the use of a GLAO system with an adaptive secondary for FALCON.

2.3. FALCON concept

Our approach is to keep the global tomographic aspect used in MCAO: it ensures to perform a good phase reconstruction wherever in the field, but we will compensate the phase locally for each tiny scientific object. This lead to an instrument where the full VLT Nasmyth field of view is to be crowded with:

– 60 small wavefront sensors, analyzing the perturbation all across the field thanks to the available bright ($m_R < 17$) stars lying there;
– 20 integral field units (IFUs), that are tiny electrooptical devices spotting at the galaxies, correcting the wavefront, and forming the sharp, corrected image, onto a microlens array. These microlenses sample the field: they split the galaxy image and properly feed IR fibers that send the IR light to the spectrograph(s). These adaptive microdevices are driven by a control computer. This latter uses the measurements from 3 to 60 wavefront sensors to perform a global 3-D phase reconstruction, and project it on each adaptive micromirror.

We began the study considering only the use of natural guide stars (NGS). This point of view might be discussed, but we believe that using a Laser Guide Star (LGS) [15,16], although a very attractive and easy solution at first sight, could be difficult to implement (there are a minimum of 20 beacons) and generates other problems, such as cone effect [17], beacon elongation, superposition of Rayleigh scattering and beacons, etc. Our approach is to base the system on NGS. If the simulation show that it fails, then the LGS option will be studied.

This system differs from classical AO systems in many ways, but the most dramatic is that it has to work in open-loop: the wavefront sensors have no feedback from the action of the adaptive microcomponents in the IFUs. This is certainly one of the main technical challenge of this instrument. The other challenge is undoubtedly that these system have to be miniaturized: the diameter of the components (wavefront sensors and corrective devices) should not exceed a typical size of 20 mm, equivalent to approximately 30 arcsec on the sky.

2.4. The open-loop working mode

We have initiated a research program to address the open-loop issues.

In order to attack the 'open loop working mode', two main ideas were in competition:

(i) make efforts to find or manufacture reliable, high accuracy open-loop components (mirror and sensor), with smart calibration procedures, in order to work in a real, actual open-loop way;
(ii) find a way to inject an optical feedback from the mirror to the wavefront sensors, so that the loop could be partially closed [19].

We first started with the second option, trying to integrate in the wavefront sensor a micromirror whose commands could have been those (or a function of those) applied to the scientific target. Although promising at first sight, this option is now abandoned due to an exponentially increased complexity.

We then turned to the first option, and we used a measurement bench to test some electrostatic mirrors.

The bench, developed by the Laboratoire d'astrophysique de Marseille (LAM), has been developed in a framework wider than FALCON, for the characterization of micromirrors. It is a high-resolution and low-coherence Twyman–Green interferometer, with different magnification configurations, either for very sharp (approx. 4 µm transversal resolution) analysis of the micro-mirror structure, or for a whole device study (with sizes up to 40 mm). The measurement technique uses a $\pi/4$ phase modulation, and the whole bench is protected from air turbulence and vibrations. This leads to a remarkable accuracy much below 1 nm rms.

The OKO electrostatic mirrors [20] are membrane mirrors, driven by the electrostatic force, and they were sounded out as good candidates for an open-loop operation since there is no reason for hysteresis to appear. This is what this bench-tests could demonstrate [21], as it was possible to derive a model allowing us to predict the behavior of the mirror, with respect to the voltage applied, with an accuracy better than 10 nm rms. This result is far below that required. Although these mirrors appear to us to have a too limited stroke and cannot be used on a real instrument [22], they demonstrate that this kind of technology could allow a real open-loop operation, provided proper calibrations and drifts are under control. We now plan to extend our tests to different types of micromirrors, such as those developed by FLORALIS (magnetic actuation) [23], or at LAM-LAAS (electrostatic) [24].

In parallel to this, we develop a high dynamic range wavefront sensor, able to provide reliable open-loop measurements while using a minimum number of pixels. This latter requirement is imposed to us by the miniaturization constraints. We follow two parallel developments:

– our first approach is to use a 'classical' Hartmann–Shack wavefront sensor together with some smart image processing algorithms, in order to increase the dynamics while keeping a reasonable number of pixels [25];
– the second is to investigate the possibility of a pyramid wavefront sensor, optimized for wide dynamic range thanks to an adequate beam modulation: the advantage of this is to use only 4 pixels per measurement, which is probably the minimum possible value for measuring a phase gradient.

Another promising solution is to use the optical differentiation wave-front sensor proposed by [26], although it seems difficult to miniaturize at first sight.

Finally, for both approaches, we work on a way to transport the image (once the wavefront sensor has encoded the phase into intensity information) through optics fibers, with no light loss (optimized injection of light in the fibers), as we feel that integrating a low-noise detector close to the WFS optics would go against miniaturization constraints.

3. Simulations

We have developed a simulation tool that computes a corrected point-spread function (PSF) at different wavelengths with a tomographic method [27]. We have assumed a 8-meter telescope and a seeing of 0.81 arcsec at 0.5 µm (median seeing at Paranal), leading to r_0 (the Fried parameter [28]) of 12.7 cm. The turbulence profile includes 3 layers at altitudes of 0, 1 and 10 km with respectively 20%, 65% and 15% of the total phase variance, leading to an isoplanatic angle $\theta_0 = 2.42$ arcsec at zenith (median isoplanatic angle at Paranal). The phase screens of the turbulent layers were simulated by Fourier-filtering methods with a correction of low-order modes in order to properly manage the effects of the outer scale of turbulence. This latter has been set to $L_0 = 25$ m, the median value [29] for Paranal.

A sample of 100 guide star triplets with $m_R < 17$, coming from a real cosmological field at a high galactic latitude ($b \approx 90°$) was used. For each configuration, on-axis AO corrected PSF at 0.9, 1.25 and 1.65 µm (I, J and H bands) were computed. We applied a correction of Zernike polynomials [30] ranging from radial order 1 to 14 ($2 < i < 120$).

We assumed that we are in a regime dominated by photon noise. In this case, the noise variance is proportional to N_{ph}^{-1} [31], where N_{ph} is the number of photoelectrons per frame. A wavefront slope sensor was considered (Hartmann or pyramid), leading to a propagated noise variance on Zernike polynomials following a law [31] in $(n+1)^{-2}$. We did not make any assumption about technical parameters such as optical throughput, detector noise or quantum efficiency. Instead, we defined the performance of the sensor as follows: it has a noise of 250 rd^2 at magnitude m_{lim}, this latter being the limiting magnitude (a star with $m > m_{\mathrm{lim}}$ cannot be used to close the loop). We chose either $m_{\mathrm{lim}} = 16$ or 17 in the following simulations. The value of 250 rd^2 is quite arbitrary; this is a value for which noise is roughly equal to the turbulence variance. It has been chosen like this as it corresponds to the performance of the visible wavefront sensor of the NAOS instrument [32]. Only spatial aspects of phase reconstruction were studied; no temporal error was introduced.

3.1. Discussion on the coupling factor

We emphasize the fact that common parameters such as the Strehl ratio (SR) or full width at half maximum (FWHM) are not suitable to describe the efficiency of adaptive optics, when working with integral field spectroscopy. What we want here is to maximize the flux in each pixel, in order to gain in signal-to-noise ratio on one hand, and avoid flux contamination from the neighboring pixels (to avoid signal quantum noise). For each simulated PSF, we have computed what we call *coupling factor*: it is the fraction of light, normalized to the total flux, ensquared in an aperture of 0.25×0.25 arcsec^2. This number of 0.25 arcsec comes from high-level scientific requirements, this is the typical size of the giant HII forming regions we want to observe at $z = 0.2$ to 2, i.e. this is the resolution we expect (hence we assume the use of a $0.125''$ pixel pitch).

When the aperture area tends towards 0, the coupling factor tends to the SR value. In classical imaging, the pixel size is chosen to $\lambda/2D$ for Nyquist sampling reasons. We should notice that in integral field spectroscopy in general, the pixel size is much larger; in our case it is 3 to $5\lambda/D$. The image is undersampled; this is mandatory, as a smaller pixel would lead to a deplorable signal-to-noise ratio. As an example, those galaxies just could not be detected on a diffraction-limited 8-m telescope in 8 hours integration time with $R = 10\,000$, if sampled at the Nyquist frequency.

3.2. Results

Fig. 1 shows the median value (over the 100 guide star triplets) of the coupling factor, in terms of the number of corrected Zernike terms. The figure on the left assumes a wavefront sensor with a R limiting magnitude $m_{\mathrm{lim}} = 16$, the other figure is for a better wavefront sensor, with $m_{\mathrm{lim}} = 17$ (NAOS-like). On each figure, 3 plots have been reported; they correspond to galactic latitudes of 30, 60 and 90 degrees. One has set to 40% the required coupling factor, and shown the number of Zernike terms to be corrected. The global shape of these curves should be noticed: they still significantly increase, even at high number of corrected modes. For a WFS of a moderate quality (low m_{lim}), 70 to 120 actuators are required. With a higher limiting magnitude, the correction order should be only 65 to 85 actuators to perform the same: the better the WFS, the lower should be the correction order: there is a transfer of the phase error between these two posts. Of course, the right trade-off is to balance the error budget, and the final choice depends on the technical choice of the components.

3.3. Discussion on the results of the simulations

Notice that the behavior of the coupling factor versus i (i is the number of compensated modes) is quite unusual. The FWHM saturates quickly to the diffraction limit value. The SR saturates too: it behaves as $(1 - \sigma_\phi^2)$ and the variance of high-order modes σ_ϕ^2 is known to be small: hence the weak variation versus i. The coupling factor has a different behavior: it still significantly increases with the number of corrected modes, and the reason is that, for a fixed amount of phase variance removed, high-order modes compensation is particularly effective at 'gathering' the light close to the PSF center, in the aperture. It is much more effective than for low-order modes. That is why when $SR(i)$ or $FWHM(i)$ rather tend to saturate, the coupling factor still increases.

The consequence is that a rather large number of actuators is required, compared with the moderate resolution required (approx. 0.25 arcsec): one has to bring the light from the further parts of the halo back to somewhere close to the center, and only a high-order modes compensation can allow this.

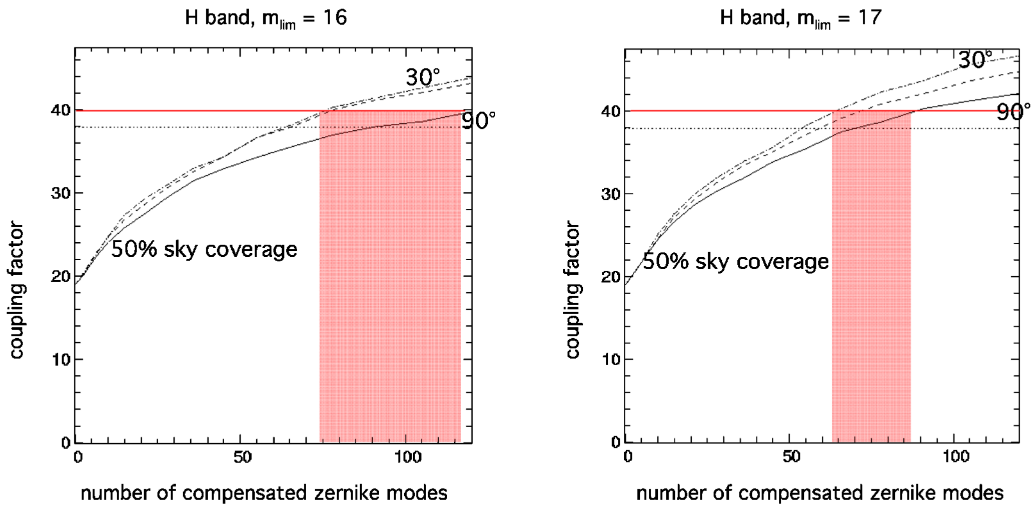

Fig. 1. Both figures show the median value, over 100 different triplets, of the simulated coupling factor in terms of the number of compensated Zernike modes. The 3 curves apply to different galactic latitudes. The left figure is for a wave-front sensor with a limiting magnitude of $R = 16$, the right one for $R = 17$. This shows that, depending on the conditions, 60 to 100 zernike modes are required to achieve a goal of 40% coupling factor.

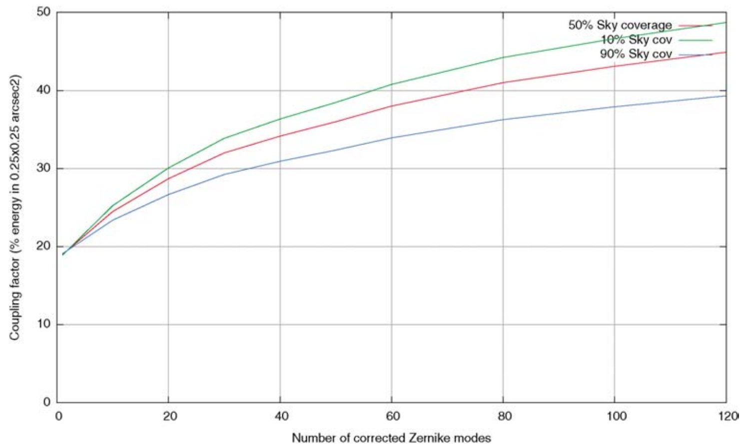

Fig. 2. The figure shows the coupling factor versus the number of compensated Zernike modes, for 3 different sky coverages. One can see that the dispersion of the coupling factor performance is rather small around the median value.

3.4. Sky coverage issues

One should notice also that the plotted results (Fig. 1) are a median value of the coupling factor, computed over the 100 triplets. This means that the performance will be better than shown for 50% cases, and worse for the other 50%. In other words, it means that the performance shown here stands for a sky coverage of 50%.

Immediately a question arises, that is to know whether 50% sky coverage is a sufficient percentage, or not. This seems to be a critical issue, as demonstrated by Fig. 2: the coupling factor has been plotted in terms of the number of corrected Zernike modes, for sky coverage of 10, 50 and 90%. For a goal of 40% in coupling factor, we can see that the number of Zernike modes should respectively be 55, 75, or 130.

This way of thinking leads to the terrible conclusion that the design of the system is dramatically dependent of the sky coverage. However, this is only partly true, because a sky coverage of 50% does not mean that only half of the objects can be observed while the others are not accessible. The right interpretation is that 50% of the objects are observable (some of them with an even better quality than expected), and most of the other 50% are observable too, but with a moderate image quality. This latter could, however, be sufficient: although lower than the expected goal, it will be, in any case, much better than the uncompensated seeing.

As an example, when assuming a goal of 40% coupling factor, one has to compensate 75 Zernike modes, to get 50% sky coverage. In these conditions, 95% of the galaxies can be observed with a performance ranging between 36% and 43% coupling factor. In other words, the dispersion of the performance in coupling factor is low. This makes the 50% sky coverage a very acceptable performance.

We shall also notice that we will have a relative variation of ±15% in the coupling factor across the different objects in the field. This strongly suggests to perform an estimation of the PSF from the environment parameters (seeing, $C_n^2(h)$, wind speed, star geometry) and wave-front sensor measurement in order to be able to unbias the data from PSF effects, by modeling or deconvolution.

4. Conclusions

The proposed concept is to correct only small areas of a few arcseconds (distant galaxy size), spread in a wide field of view, assuming specific adaptive optics systems located at or near each of the targeted galaxies. By coupling these AO systems to a spectrograph with multiple IFUs, one can improve by a factor greater than 2 the light concentration within an aperture of 0.25 arcsec, when compared to the natural seeing conditions, and observe simultaneously up to 20 galaxies.

Our simulations show that a system with approximately 80 actuators in the pupil (10 × 10 actuators), relying on 3-stars tomography and using NGS only:

– can reach a spatial resolution much better than 0.25 arcsec, in J and H, for 95% of the objects;
– can achieve a coupling factor larger than 40% in H for 50% of the objects (initial scientific goal);
– can achieve a coupling factor larger than 34% in H for 95% of the objects;
– cannot observe, or only with a marginal improvement, less than 5% of the objects.

If implemented at VLT, this system has to include very small devices to avoid field obstruction. These are the main drawbacks: such devices require a new generation of micro deformable mirrors and miniaturized wavefront sensors. Another critical issue is the need to 'partially' close the AO loop, or work in open loop.

The FALCON concept can be extrapolated to Extremely Large Telescopes (ELTs). Indeed cosmological studies in the very distant Universe require reasonably large fields of view to study galaxy formation at scales beyond the typical lengths of galaxy correlation. Simple extrapolations suggest that FALCON would make possible to detail galaxy physics down to 400 pc scales at $z = 2$–6, and then to describe in details the mechanisms of the formation of each present day galaxy type. Miniaturization of the FALCON devices might be somewhat relaxed, although to reach such exquisite spatial resolutions would require a significantly larger number of actuators per deformable mirror. We believe that ELTs equipped with FALCON would be unbeatable to understand how galaxies were formed since the epoch of re-ionization and beyond.

Acknowledgements

Our study of the FALCON concept is supported by contracts with the Paris Observatory, CNRS and ESO. We also thank the referee for very valuable comments.

References

[1] P. Amram, J. Boulesteix, M. Marcelin, C. Balkowski, V. Cayatte, W.-T. Sullivan, Hα velocity fields and rotation curves of galaxies in clusters III. Nine galaxies in DC 1842-63, Astron. Astrophys. S 113 (1995) 35.
[2] K.L. Adelberger, C.C. Steidel, M. Giavalisco, M. Dickinson, M. Pettini, M. Kellogg, A counts-in-cells analysis of Lyman-break galaxies at redshift $z \approx 3$, Astrophys. J. 505 (1998) 18.
[3] Labbé, et al., Ultradeep near-infrared ISAAC observations of the Hubble Deep Field South: observations, reduction, multicolor catalog, and photometric redshifts, Astrophys. J. 587 (2003) 83.
[4] M. Pettini, M. Kellogg, C. Steidel, M. Dickinson, K.L. Adelberger, M. Giavalisco, Infrared observations of nebular emission lines from galaxies at $z \approx 3$, Astrophys. J. 508 (1998) 539.
[5] D.L. Fried, Anisoplanatism in adaptive optics, J. Opt. Soc. Am. A 72 (1982) 52.
[6] R.H. Dicke, Phase-contrast detection of telescope seeing errors and their correction, Astrophys. J. 198 (1975) 605.
[7] J.M. Beckers, Increasing the size of the isoplanatic patch with multiconjugate adaptive optics, in: M.H. Ulrich (Ed.), ESO Conf. on Very Large Telescopes and their Instrumentation, ESO Conference and Workshop Proceedings, vol. 2, 1989, p. 693.
[8] T. Fusco, J. Conan, V. Michau, L.M. Mugnier, G. Rousset, Phase estimation for large field of view: application to multiconjugate adaptive optics, in: M.C. Roggemann, L.R. Bissonnette (Eds.), Propagation and Imaging through the Atmosphere III, in: Proc. SPIE, vol. 3763, 1999, p. 125.

[9] M. Le Louarn, Multi-conjugate adaptive optics with laser guide stars: performance in the infrared and visible, Mon. Not. R. Astron. Soc. 334 (865) (2002) 22.
[10] R. Ragazzoni, E. Marchetti, F. Rigaut, Modal tomography for adaptive optics, Astron. Astrophys. 342 (1999) L53.
[11] A. Tokovinin, M. Le Louarn, E. Viard, N. Hubin, R. Conan, Optimized modal tomography in adaptive optics, Astron. Astrophys. 378 (2001) 710.
[12] A. Tokovinin, E. Viard, Limiting precision of tomographic phase estimation, J. Opt. Soc. Am. A 18 (2001) 873.
[13] E. Marchetti, R. Brast, B. Delabre, et al., MAD status report, in: Advancements in Adaptive Optics, in: Proc. SPIE, vol. 5490, 2004, p. 236.
[14] B.L. Ellerbroek, F.J. Rigaut, B.J. Bauman, C. Boyer, S.L. Browne, R.A. Buchroeder, J.W. Catone, P. Clark, C. d'Orgeville, D.T. Gavel, G. Herriot, M.R. Hunten, E. James, E.J. Kibblewhite, I.T. McKinnie, J.T. Murray, D. Rabaud, L.K. Saddlemyer, J. Sebag, J. Stillburn, J.M. Telle, J. Veran, Multiconjugate adaptive optics for Gemini-South, in: P.L. Wizinowich, D. Bonaccini (Eds.), Adaptive Optical System Technologies II, in: Proc. SPIE, vol. 4839, 2003, p. 55.
[15] R. Foy, A. Labeyrie, Feasibility of adaptive telescope with laser probe, Astron. Astrophys. 152 (1985) L29.
[16] M. Le Louarn, R. Foy, N. Hubin, M. Tallon, Laser Guide Star for 3.6- and 8-m telescopes: performance and astrophysical implications, Mon. Not. R. Astron. Soc. 295 (1998) 756.
[17] M. Tallon, R. Foy, Adaptive telescope with laser probe – isoplanatism and cone effect, Astron. Astrophys. 235 (1990) 549.
[18] N. Hubin, et al., Ground Layer Adaptive Optics, C. R. Physique 6 (2005), in this issue.
[19] M. Puech, F. Chemla, P. Laporte, et al., Deformable mirrors for the FALCON concept, Astronomical Adaptive Optics Systems and Applications II, Proc. SPIE, vol. 5903, 2005, in press.
[20] G.V. Vdovin, Optimization-based operation of micromachined deformable mirrors, in: Adaptive Optical System Technologies, in: Proc. SPIE, vol. 3353, 1998, p. 902.
[21] A. Liotard, F. Zamkotsian, Static and dynamic micro-deformable mirror characterization by phase-shifting and time averaged interferometry, International Conference on Space Optics (ICSO) 2004, Toulouse, France, March 2004.
[22] Paterson, et al., in: Adaptive Optical Systems Technology, in: Proc. SPIE, vol. 4007, 2000, p. 185.
[23] J. Charton, Z. Hubert, E. Stadler, W. Schartz, J.-L. Beuzit, in: Atad-Ettedgui, D'Odorico (Eds.), Specialized Optical Developments in Astronomy, in: Proc. SPIE, vol. 4842, 2003, pp. 207–218.
[24] F. Zamkotsian, V. Conedera, A. Liotard, A. Schroeder, N. Fabre, P. Lanzoni, H. Camon, Polymer-based microdeformable mirror for adaptive optics, in: SPIE Conference MOEMS 2005, San Jose, USA, January 2005, Proc. SPIE, vol. 5719.
[25] R. Lane, M. Tallon, E. Thiébaut, R.M. Clare, Diffraction limited image restoration by post-compensation from simultaneous speckle and wavefront sensing observations, in: P.L. Wizinowich, D. Bonaccini (Eds.), Adaptive Optical System Technologies II, in: Proc. SPIE, vol. 4839, 2003, pp. 1142–1153.
[26] J.E. Oti, V.F. Canales, M.P. Cagigal, Improvements on the optical differentiation wavefront sensor, Mon. Not. R. Astron. Soc. 360 (2005) 1448.
[27] F. Assémat, et al., FALCON: a new generation spectrograph with adaptive optics for the ESO VLT, in: Optics in Atmospheric Propagation and Adaptive Systems VI, in: Proc. SPIE, vol. 5237, 2003, p. 221.
[28] D.L. Fried, Optical resolution through a randomly inhomogeneous medium for very long and very short exposures, J. Opt. Soc. Am. 56 (1966) 1372.
[29] F. Martin, R. Conan, A. Tokovinin, A. Ziad, H. Trinquet, J. Borgnino, A. Agabi, M. Sarazin, Optical parameter relevant for high angular resolution at Paranal from GSM instrument and surface layer contribution, Astron. Astrophys. Suppl. Ser. 144 (2000) 39–44.
[30] R.J. Noll, Zernike polynomials and atmospheric turbulence, J. Opt. Soc. Am. A 66 (1976) 207.
[31] F. Rigaut, E. Gendron, Laser guide star in adaptive optics – the tilt determination problem, Astron. Astrophys. 261 (1992) 677.
[32] G. Rousset, F. Lacombe, P. Puget, N. Hubin, E. Gendron, T. Fusco, et al., NAOS, the first AO system of the VLT: on-sky performance, in: P.L. Wizinowich, D. Bonaccini (Eds.), Adaptive Optical System Technologies II, in: Proc. SPIE, vol. 4839, 2003, pp. 140–149.